P3-18

Turbulent transport and the scrape-off-layer width

J.R. Myra,[a*] D.A. Russell,[a] D.A. D'Ippolito,[a] J-W. Ahn,[b] R. Maingi,[b] R.J. Maqueda,[c,d] D.P. Lundberg,[d] D.P. Stotler,[d] S.J. Zweben,[d] M. Umansky[e]

[a] *Lodestar Research Corp., Boulder, Colorado, USA*

[b] *Oak Ridge National Laboratory, Oak Ridge, Tennessee, USA*

[c] *Nova Photonics, Inc., Princeton, New Jersey, USA*

[d] *Princeton Plasma Physics Laboratory, Princeton, New Jersey, USA*

[e] *Lawrence Livermore National Laboratory, Livermore, California, USA*

The two-dimensional fluid turbulence code SOLT is employed to study the role of midplane turbulence on the scrape-off-layer (SOL) heat flux width of tokamak plasmas. The physics simulated includes curvature-driven-interchange modes, sheath losses, and perpendicular turbulent diffusive and convective (blob) transport. Midplane SOL profiles of density, temperature and parallel heat flux are obtained from the simulation and compared with experimental results from the National Spherical Torus Experiment [NSTX] to study the scaling of the heat flux width with power and plasma current. It is concluded that midplane turbulence is the main contributor to the SOL width for the low power ELM-free H-mode discharges studied, while additional physics is required to explain the plasma current scaling of the SOL width observed experimentally in higher power discharges. Additional simulations predict a transition to a convectively-dominated SOL at critical values of power and connection length.

JNM keywords: Theory and Modeling, Plasma Properties

PSI-19 keywords: SOL transport, Plasma turbulence, NSTX, Power flux

PACS: 52.55.Fa, 52.35.Ra, 52.65.-y, 52.40.Kh

**Corresponding author address:* Lodestar Research Corporation

2400 Central Ave., P-5

Boulder, Colorado, USA 80301

**Corresponding author e-mail:* jrmyra@lodestar.com

Presenting author: James R. Myra

Presenting author e-mail: jrmyra@lodestar.com

1. Introduction

Understanding the physical processes that control the radial width of the scrape-off-layer (SOL) is a key issue for the tokamak and spherical torus concepts. It is well known that future devices may be constrained by the power flux impacting material surfaces. [1] Moreover, the particle flux influences fueling through recycling. In this paper we report on recent progress in theory, simulation and the comparison of these with data, on the characteristics of the SOL.

The SOL width is set by a competition between cross-field and parallel transport. In the present model, we consider the role of electrostatic turbulence at the midplane on the cross-field transport fluxes and midplane profiles. Midplane turbulence gives rise to fluctuating $\mathbf{E} \times \mathbf{B}$ convection near the last closed surface (LCS) which can result in both diffusive and convective transport processes. We have previously studied [2, 3] the role of convective transport by coherent structures, i.e. blob-filaments [4], in the far SOL. In addition to their interest for basic physics, and for model validation, these studies are relevant to practical issues such as wall damage and wall recycling. To address the issue of power flux on the divertor plates, transport in the near SOL is of most interest, and that region is the main focus of the present paper. Here, depending on parameters, both convective and diffusive mechanisms can compete.

Conceptually, we can follow the flow of power in two steps: first across the separatrix on the outboard side of the torus, and then along field lines through the X-point region and divertor leg to the target plate. Similar to a related experimental study on the role of convective transport in establishing the SOL density width [5], we assume here that the parallel transport is governed by classical processes. The goal of the present study is to apply a simulation model, described in Sec. 2, for the turbulent-induced cross-field transport and SOL profiles at the outboard midplane and use it to predict the resulting heat deposition footprint on the divertor plate. In Sec. 3.1 and 3.2, we will apply this model to two sets of discharges in the National Spherical Torus Experiment [NSTX] [6] which address the power and plasma current scaling of the SOL width.

Additional simulations in Sec. 4 show predicted theoretical scalings with connection length and an interesting transition in the turbulent dynamics.

2. Simulation code and technique

The computation tool used for these studies is the Scrape-Off-Layer Turbulence (SOLT) code, which is described in detail in recent publications [7]. Briefly, SOLT is a two-dimensional fluid turbulence code which models the plane perpendicular to the magnetic field B in the outboard midplane of the torus. SOLT implements classical parallel physics using closure relations [4] for the midplane parallel current and parallel fluxes for collisional regimes ranging from sheath-connected to conduction limited. In the present paper, the regime is essentially sheath-connected. The SOLT code can describe arbitrarily strong nonlinear plasma dynamics ($\delta n/n \sim 1$), including blob formation, and the physics model supports interchange-type curvature-driven modes, sheath instabilities, and drift waves. For comparison with experimental gas puff imaging (GPI) data [8], SOLT includes a synthetic GPI diagnostic which has recently been upgraded to simulate both He and D puffs.

To maintain the edge (i.e. inside the LCS) plasma profiles in the presence of SOL losses, SOLT has flexible sources for plasma density, temperature, and flows (n_e, T_e, v_y). In the present work, artificial sources for n_e and T_e are configured to maintain the experimentally observed profiles in the steep pedestal region. These artificial sources are set to zero for $r > r_{sep} - \Delta$, where we typically choose $\Delta \sim 1$ cm (comparable to the size of local turbulent structures). The main point is that the SOL profiles themselves are determined self-consistently by the balance between perpendicular turbulent transport and parallel losses.

The SOLT physics model generates both mean, $\langle v_y \rangle$, and oscillating zonal flows [ZFs] self-consistently from the action of Reynolds stress, blob dynamics and SOL sheath fields. The self-consistent ZFs are found to regulate turbulence in our simulations [7] and seem to describe L-mode experiments well [2,3]. In the H-mode discharges considered in this paper, additional turbulent regulation must be present, since the H-mode edge profiles are steeper, but the

observed turbulent fluxes are smaller than in L-mode. Here, the additional turbulent regulation is simulated by imposing a mean ZF in the edge region (not in the SOL) whose radial profile is taken to be proportional to the ion diamagnetic drift. This imposes an E_r well inside the LCS which regulates the turbulence. To simulate the H-mode discharges, the depth of the E_r well is adjusted so that the turbulent power flux across the LCS, P_{sep}, matches the corresponding experimentally measured power. Because of the use of artificial source terms for n_e, T_e and v_y, we do not regard the present simulations as applying to the region inside the LCS. Rather, what we have is a SOL simulation, with a heat-flux driven boundary condition at the separatrix, which allows the separatrix values of n_e and T_e to be unconstrained.

3. Results and comparison with NSTX

For the simulations, the following inputs are taken from the experiment: power crossing the separatrix P_{sep}, connection length from the midplane to the divertor plate in the SOL $L_{||}(r)$, plasma profiles inside the LCS $n_e(r)$ and $T_e(r)$ for $r - r_{sep} < \Delta$ and R, B_t and B_p at the outboard midplane. These data determine the gradient drive for instability, the toroidal curvature, the collisionality regime, and indirectly the turbulent-driven heat-flux crossing the SOL. Other code inputs include dissipation parameters, primarily viscosity, and downstream plasma conditions at the divertor plate, assumed here to match those at the midplane (in the sheath connected regime).

From the simulations, we can compare key outputs with experiment, such as the mean parallel heat flux $\langle q_{||}(r)\rangle$, and its width λ_q, (vs. midplane-mapped data from the IR cameras), the SOL profiles $\langle n_e(r)\rangle$ and $\langle T_e(r)\rangle$ (vs. midplane reciprocating probe data) and 2D snapshots or movies of the turbulence (simulated vs. experimental midplane GPI).

Simulation results are presented here in terms of simulation power scans, where the imposed flows are varied and the resulting simulated P_{sep} determined from

$$P_{sep} = 2\pi R b_\theta \int dr\, q_{||} \qquad (1)$$

where $b_\theta = B_p/B$ and the integral is taken across the entire SOL. The simulation point where P_{sep} most closely matches the experimental value is employed for comparison. It is important to

point out that these simulation power scans hold other simulation inputs fixed (such as pedestal profiles), so they do not necessary correspond directly to experimental power scans.

3.1 Low power ELM-free H-mode

We first examined two low power ELM-free H-mode discharges [9] at different neutral beam power levels: NSTX shot 135009 at P_{nb} = 0.8 MW and shot 135038 at P_{nb} = 1.3 MW. For these shots midplane probe data were available for comparison with the simulations. Results for the simulation power scan are shown in Fig. 1. In this case, there were apparently insignificant differences in the SOLT setup for the two shots, so the power scans overlay within scatter. The solid line is a linear fit to the combined simulation data. The gray ellipses correspond to the experimental powers. From the fit, we can deduce the simulated scaling of λ_q with P_{sep} and compare with experimental data (see Table 1). All experimental widths in the table are mapped to the midplane.

The experimental profiles of $q_{||}(R\text{-}R_{sep})$ measured at the divertor plate show some broadening into the private flux region $R < R_{sep}$, (width λ_{qPriv}) as well as into the main SOL, $R > R_{sep}$ (width λ_{qSOL}) . The presence of the exhaust plasma in the private SOL is indicative of perpendicular transport processes occurring between the X-point and the plate. These are not included in the SOLT model. To account for this heuristically, as well as any heat diffusion on the divertor plate itself that might affect the measurement of $q_{||}$, Table 1 displays the difference between the measured λ_q on the main SOL side and private flux regions, i.e. $\lambda_{q1} \equiv \lambda_{qSOL} - \lambda_{qPriv}$. In some strictly diffusion-based models, a quadrature subtraction, denoted $\lambda_{q2} = (\lambda_{qSOL}^2 - \lambda_{q\,Priv}^2)^{1/2}$ may provide a better correction. [10] In any case, both simulation and experiment show a weak positive scaling of λ_q with power.

Comparison of the simulation and midplane probe data for n_e and T_e will be presented elsewhere. The level of agreement is generally within the scatter of the experimental measurements, except for n_e near the separatrix where SOLT overestimates by about 50%. ($T_{e,sep}$ agreement is better.) We speculate that the reason may be due to a 3D effect that is not

modeled in SOLT: blob-filaments crossing the separatrix should expand along the field lines to fill the longer SOL flux tube. If negligible work is done in this parallel sonic expansion, the result would be a reduction in midplane density at constant temperature.

3.2 Scaling of the SOL width with plasma current

A similar analysis was carried out for two shots at higher power (P_{nb} = 6 MW) and different plasma currents [11]: NSTX shot 128013 at I_p = 0.8 MA and shot 128797 at I_p = 1.2 MA with B_t approximately constant. Results for the simulation power scans are shown in Fig. 2. These SOLT simulations take account of the difference in connection length $L_{||}(r)$, B_p and pedestal n_e and T_e profiles for the 2 shots as well as small differences in P_{sep} and B_t. The narrow gray ellipses denote the experimental P_{sep} for the two shots. The connection length affects the slope of λ_q vs. P_{sep} in the two cases directly through the B_p/B factor in Eq. (1) and indirectly through the parallel loss terms in the SOL turbulence equations.

A measurable broadening of the SOL width is predicted by the simulations for the lower I_p case. Simulation and experimental results are quantified in Table 2. Again, all experimental widths in the table are mapped to the midplane. Here λ_{qexp} is the $q_{||}(r)$ width on the main SOL side of the peak, as fitted by an exponential and λ_{qint} is the width determined by the integral method, i.e. using Eq. (1) and the peak heat flux $P_{sep} = 2\pi R b_\theta \lambda_{q\,int} q_{||peak}$. No matter which measure of λ_q is employed, the inverse scaling of λ_q with I_p is much stronger in the NSTX experimental data than in the SOLT simulations.

Two possibilities can be proposed to understand the discrepancy: (i) the SOLT physics model is not giving the correct dependence of the midplane turbulence on I_p, or (ii) mechanisms other than midplane turbulence are required to explain the broadening of λ_q in the low I_p case. To help decide between (i) and (ii) we compared the midplane GPI data with SOLT simulated GPI for the two shots. This comparison showed that midplane turbulence levels as characterized by $\delta I/I$ are similar for the two shots in both NSTX and SOLT. Details will be reported elsewhere.

As a result, hypothesis (ii) appears to be favored. Possible mechanisms include divertor leg instabilities [12], ELM and MHD effects which could cause strike point motion [13], and X-point loss of ions due to drift-orbit effects [14] which might be expected to be a particularly strong effect at low I_p. Caveats in our analysis include possible differences in downstream sheath conditions for the two shots and MHD activity not included in these electrostatic simulations.

4. Transition to a convectively dominated SOL

Additional simulations have been carried out to study the scaling of the SOL width and properties of the turbulence when varying the inputs of the simulation one at a time. For the set of studies described here, we used shot 135009 as a base case and artificially varied $L_{||}$ to study the theoretical scaling of λ_q with connection length. Unlike the I_p scaling study which also varies connection length, here we held the pedestal profiles fixed, and were able to change $L_{||}$ by a larger factor.

For a diffusive SOL, the scaling $\lambda_{diff} \sim (D\tau_{||})^{1/2} \propto L_{||}^{1/2}$ might be expected, while if perpendicular convective transport dominates, we would expect $\lambda_{conv} \sim V\tau_{||} \propto L_{||}$ where we assume the parallel physics is dominated by convection with characteristic time $\tau_{||} \sim L_{||}/v_{||}$. Figure 3 compares a simulation power scan for the base case (same data as in Fig. 1) with a case that has double the connection length, $L_{||} = 2L_{||0}$. The resulting values of λ_q have been renormalized taking out the factor $(L_{||0}/ L_{||})^{1/2}$. The results show a transition from diffusive to convective scaling of the near-SOL width when P_{sep} and $L_{||}$ exceed critical values.

In the diffusive regime, the near-SOL width is determined by intermittent separatrix-spanning convective cells, while strong blob emission and increasing frequency of bursts dominates the SOL width in the convective regime. Preliminary analysis suggests that the diffusive-convective transition occurs when $k_y\lambda_q > 1$ where k_y is the dominant spectral component of the turbulence in the binormal direction. This is consistent with simple heuristic arguments. Estimating the diffusion coefficient as $D \sim \gamma / k_y^2$ with γ the linear growth rate, and the blob velocity as $v_b \sim \gamma/k_y$ [4] and defining the blob packing fraction f_p, we find the ratio of

diffusion to convection $D\nabla \ln n$: $v_b f_p$ scales as $1/ k_y L_n$: f_p. As L_n increases with power, diffusion becomes ineffective and gives way to convection at ever increasing packing fraction (burst frequency).

5. Discussion and conclusions

Although it is reassuring that the simulated values of λ_q in Sec. 3 are comparable to the experimental ones, absolute agreement is not the point of these simulations. Sensitivity of the simulated results to input parameters (especially experimentally unknown dissipative terms like viscosity) prevents taking the absolute numbers too seriously. Also, the inherent nature of 2D simulations (where scalar parameters represent averages over the parallel dimension) limits the expected accuracy of results. Instead our main focus is on capturing the trends that can be expected when interchange-like **E**×**B** turbulent transport dominates the SOL physics.

Comparison with experimental data for n_e, T_e, and $q_{||}$ in low-power ELM-free H-modes suggests that midplane interchange-like turbulence is the main contributor to the λ_q width in this scenario and results in a weak positive power scaling. In contrast, the experimentally observed strong I_p scaling of λ_q from NSTX data is not seen in SOLT simulations, and suggests the importance of other mechanisms, especially at low I_p.

In a theoretical simulation study, we showed a transition from diffusive to convective scaling for the near-SOL width for critical values of power and connection length.

Several other investigations have been carried out based on the SOLT simulations reported on here. In particular we have examined the emission of blobs and compared with GPI data. In NSTX, blob emission tends to be rare in H-mode, and in our simulations of these shots, blob emission typically does not occur in the absence of imposed transients. This raises the question of whether blob emission in the experiments is triggered by transient events propagating outward from the core. These and other questions remain for future study.

Acknowledgements

This work was supported by the US DOE under grants DE-FG02-02ER54678 and DE-FG02-97ER54392.

References

1. B. Lipschultz ,et al., Nucl. Fusion **47**, 1189 (2007).
2. D. A. D'Ippolito, et al., 22nd IAEA Fusion Energy Conference, Geneva, Switzerland, October 13 - 18, 2008, paper IAEA-CN-165/TH/P4-17.
3. D.A. Russell et al., Bull. APS **53**, 193 (2008), paper NP6-116; report in progress.
4. S. I. Krasheninnikov, D. A. D'Ippolito, and J. R. Myra, J. Plasma Physics **74**, 679 (2008).
5. S.J. Zweben, J.L. Terry, B. LaBombard, M. Greenwald, et al., this conference.
6. M. Ono et al., Nucl. Fusion **40**, 557 (2000).
7. D. A. Russell, J. R. Myra and D. A. D'Ippolito, Phys. Plasmas **16**, 122304 (2009); and refs. therein.
8. S.J. Zweben, R.J. Maqueda, D.P. Stotler et al, Nucl. Fus. **44**, 134 (2004).
9. J. W. Ahn et al. (private communication).
10. R. J. Goldston, Phys. Plasmas **17**, 012503 (2010).
11. R. Maingi, et. al., J. Nucl. Mater **363-365**, 196 (2007); T.K. Gray, et. al., this conference.
12. D.D. Ryutov and R.H. Cohen, Contrib. Plasma Phys. **48**, 48 (2008).
13. E. R. Solano et al., J. Nucl. Mater. **337–339** 747 (2005).
14. S. Ku, H. Baek, and C. S. Chang, Phys. Plasmas **11**, 5626 (2004).

Figure Captions

1. Simulation power scans in P_{sep} for two low power ELM-free H-mode discharges. The SOLT heat flux SOL widths λ_q are shown (filled circles) together with a linear fit to all the simulation data. Large ellipses indicate the experimental power in each case.
2. Simulation power scans for shots studying the scaling of the SOL width with plasma current. The SOLT results for λ_q are shown (filled circles) together with linear fits for each of the two shots. Ellipses indicate the experimental power in each case.
3. Theoretical study of the scaling of the heat flux width with connection length and power. Open circles are the base case λ_q and filled circles give the diffusively scaled result $\lambda_q(L_{\|0}/L_{\|})^{1/2}$ for a case with $L_{\|}$ doubled. For this case, a transition to convective scaling occurs at $P_{sep} \sim 1.3$ MW.

Figures

Fig. 1

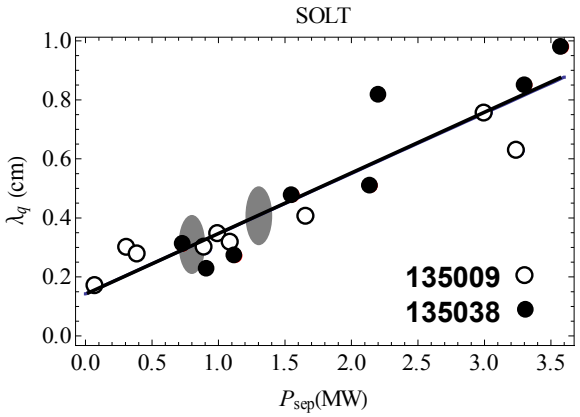

Fig. 2

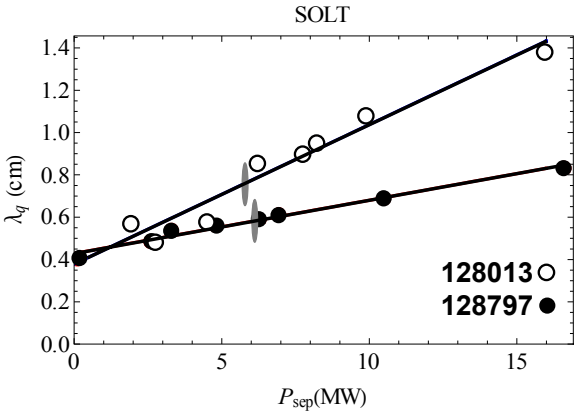

Fig. 3

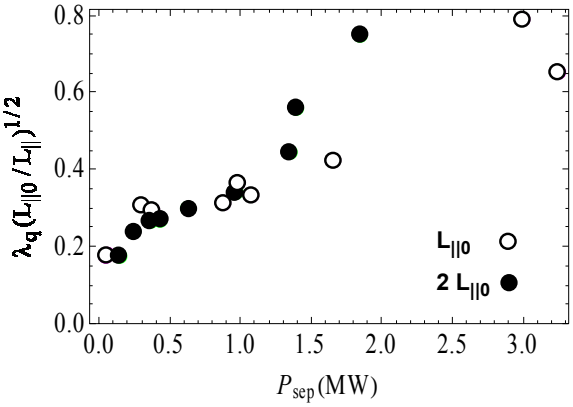

Tables

shot	P(MW)	$\lambda_{q,SOL}$(cm)	$\lambda_{q,Priv}$(cm)	λ_{q1}(cm)	λ_{q2}(cm)	λ_{qSOLT}(cm)
135009	0.8	0.57	0.21	0.36	0.52	0.30
135038	1.3	0.70	0.20	0.50	0.67	0.41

Table 1. Power scaling of the SOL width for low power ELM-free H-modes. The first 6 columns, described in the text, are from the experiment. The last column is the midplane SOL width from the SOLT simulations.

shot	I_p(MA)	P(MW)	λ_{qexp}(cm)	λ_{qint}(cm)	$\lambda_{qintSOLT}$(cm)
128013	0.8	5.8	0.65	1.73	0.76
128797	1.2	6.1	0.24	0.56	0.58
ratio	0.67	0.95	2.7	3.1	1.3

Table 2. Power scaling of the SOL width for the I_p current scan. The first 5 columns, described in the text, are from the experiment. The last column is the midplane SOL width from the SOLT simulations. The ratio of the various λ's for the two shots is also given.